Finite-Volume Solution of the Compressible Boundary-Layer Equations

Bernard Loyd* and Earll M. Murman†
Massachusetts Institute of Technology, Cambridge, Massachusetts

Abstract

A BOX-type finite-volume discretization is applied to the integral form of the compressible boundary-layer equations. Boundary-layer scaling is introduced through the grid construction: streamwise grid lines follow $\eta = y/h = \text{const}$, where y is the normal coordinate and $h(x)$ a scale factor proportional to the boundary-layer thickness. With this grid, similarity can be easily applied to calculate initial conditions. Computations for similar and nonsimilar flows are given, and show excellent agreement with tabulated results, solutions computed with Keller's box scheme, and experimental data. (Solution details and additional results may be found in Ref. 1.)

Although numerous solution schemes to the differential boundary-layer equations exist, most of these introduce equation and/or coordinate transformations that tend to obscure the physical meaning of the equations and their solutions. The finite-volume method preserves the physical transparency of the integral equations in the discrete approximation, while maintaining (and, in some cases, improving upon) the accuracy and efficiency of the best conventional methods. Thus, the authors feel that the finite-volume approach is a valuable addition and a viable alternative to existing schemes.

Contents

Finite-volume methods approximate integral forms of conservation equations on finite cells. The equations are approximated by summing the fluxes of mass, momentum, and energy from neighboring cells in each cell, thereby satisfying the conservation equations over that cell. A key part of the finite-volume approach is the decoupling of the discretization of the equations from the grid generation. The equations are first discretized for an arbitrary quadrilateral cell in the physical coordinate system. The grid is constructed to provide resolution where needed. Similarity principles are applied explicitly to calculate an initial solution.

Governing Equations

The two-dimensional steady boundary-layer equations in integral form are

$$\oint \rho u \mathrm{d}y - \oint \rho v \mathrm{d}x = 0 \tag{1}$$

$$\oint u(\rho u)\mathrm{d}y - \oint v(\rho u)\mathrm{d}x = -\oint P\mathrm{d}y - \oint \tau \mathrm{d}x \tag{2}$$

$$\oint u(\rho H)\mathrm{d}y - \oint v(\rho H)\mathrm{d}x = -\oint q\mathrm{d}x \tag{3}$$

where x is arclength along and y is distance normal to a given body. Integration is counterclockwise. u and v are tangential and normal velocities, P static pressure, ρ density, and H total enthalpy. τ and q are shear stress and total enthalpy flux:

$$\tau = (\mu_l + \mu_t)\frac{\partial u}{\partial y} \tag{4}$$

$$q = \left[\frac{\mu_l}{Pr_l} + \frac{\mu_t}{Pr_t}\right]\frac{\partial H}{\partial y} + \mu_l\left[1 - \frac{1}{Pr_l}\right]u\frac{\partial u}{\partial y} \tag{5}$$

Subscripts l and t denote laminar and turbulent quantities, and Pr is the Prandtl number. Reynolds averaging has been done for turbulent flow. The laminar viscosity is obtained from Sutherland's law, and the Cebeci-Smith model is used to calculate the turbulent viscosity. The equation of state completes the system of equations. (We nondimensionalize ρ, u, v, H, P, μ, and x and y by ρ_∞, U_∞, U_∞, U_∞^2, $\rho_\infty U_\infty^2$, $\rho_\infty U_\infty L$, and L, respectively, but this does not change the forms of governing equations or dependent relations.)

Boundary conditions may be applied in the so-called direct or inverse mode. Direct mode implies specifying the edge velocity U_e and amounts to imposing a known pressure field on the boundary layer. Alternatively, one of a number of inverse boundary conditions, for example, specified displacement thickness or wall shear, is easily applied.

Stream Function (u,ψ) Discretization

Before discretization, we replace the continuity equations by a simple stream function,

$$\mathrm{d}\psi = \rho u \mathrm{d}y - \rho v \mathrm{d}x \tag{6}$$

and also use Eq. (6) to simplify the convective terms in the momentum and enthalpy equations. The stream-function formulation is preferred because the resulting equations are simpler. Below are the final forms of the governing equations and the corresponding discrete approximations using a box-type difference stencil. Subscripts refer to the sample cell in Fig. 1.

Definition of stream function:

$$\mathrm{d}\psi = \rho u \mathrm{d}y_{x=\text{const}}, \qquad \Delta\psi_2 - \rho_2 u_2 \Delta y_2 = 0$$

Definition of shear stress:

$$\tau = (\mu_l + \mu_t)\frac{\partial u}{\partial y}, \qquad \tau_2 \Delta y_2 - (\mu_l + \mu_t)_2 \Delta u_2 = 0$$

Table 1 Laminar-flow flat-plate wall shear and displacement thickness

	Wall shear		Displacement thickness	
No. of cells	Keller	Finite volume	Keller	Finite volume
10	0.33085	0.33700	1.77121	1.69312
% error	0.363	−1.488	−2.932	1.605
20	0.33177	0.33328	1.73342	1.71353
% error	0.087	−0.368	−0.737	0.419
40	0.33199	0.33237	1.72393	1.71899
% error	0.022	−0.092	−0.185	0.102
Exact	0.33206		1.72074	

Presented as Paper 86-0436 at the AIAA 24th Aerospace Sciences Meeting, Reno, NV, Jan. 6-9, 1986; received March 18, 1986; synoptic submitted Sept. 24, 1986. Full paper available from AIAA Library, 555 W. 57th St., New York, NY 10019. Price: microfiche, $4.00; hard copy, $9.00. **Remittance must accompany order.**

*NSF Fellow, Department of Aeronautics and Astronautics. Member AIAA.

†Professor, Department of Aeronautics and Astronautics. Associate Fellow AIAA.

Definition of enthalpy flux:

$$q = [\mu_l/Pr + \mu_t/Pr_t]\frac{\partial H}{\partial y} + \mu_{l_2}[1 - 1/Pr_l]\frac{u\partial u}{\partial y}$$

$$q_2\Delta y_2 - [\mu_l/Pr_l + \mu_t/Pr_t]_2\Delta H_2 - \mu_l[1 - 1/Pr]u_2\Delta u_2 = 0$$

Conservation of momentum:

$$\oint u\mathrm{d}\psi + \oint P\mathrm{d}y + \oint \tau\mathrm{d}x = 0$$

$$u_1\Delta\psi_1 + u_2\Delta\psi_2 + u_3\Delta\psi_3 + u_4\Delta\psi_4$$
$$+ P_1\Delta y_1 + P_2\Delta y_2 + P_3\Delta y_3 + P_4\Delta y_4 + \tau_1\Delta x_1 + \tau_3\Delta x_3 = 0$$

Conservation of energy:

$$\oint H\mathrm{d}\psi + \oint q\mathrm{d}x = 0$$

$$H_1\Delta\psi_1 + H_2\Delta\psi_2 + H_3\Delta\psi_3 + H_4\Delta\psi_4 + q_1\Delta x_1 + q_3\Delta x_3 = 0$$

In these equations, all Δ terms are simple centered differences taken in a counterclockwise sense, and cell side values of the functions are linear averages:

$$\Delta y_1 = y_{i+1,j} - y_{i,j}, \qquad \Delta y_2 = y_{i+1,j+1} - y_{i+1,j}$$
$$u_1 = 0.5(u_{i+1,j} + u_{i,j}), \qquad u_2 = 0.5(u_{i+1,j+1} + u_{i+1,j}) \quad (7)$$

Note that $\Delta x_2 = \Delta x_4 = 0$ always.

This discretization provides a stable second-order-accurate approximation on an arbitrary grid. Since fluxes leaving each cell are just those entering the surrounding cells, and every flux is accounted for, the discretization identically conserves mass, momentum, and energy, and it preserves the conceptual simplicity of the governing equations.

Grid Generation

Streamwise grid lines (1 and 3 in Fig. 1) must follow the physical variation of the boundary-layer thickness $\delta(x)$. Thus, we define the outermost grid line to lie along $y_e(x) = \eta_\infty\theta_k(x)$; where $\theta_k(x)$ is the incompressible momentum thickness. η_∞ (=const) is chosen so that $y_e > \delta$. Subsequent grid lines follow $y_j = \eta_j\theta_k(x)$, where $\eta_j = \eta_{j-1} + \Delta\eta_j$, and the $\Delta\eta_j$ are chosen to give any desired spacing between grid lines. For similar flows, $\theta_k(x)$ is known from similarity; for example, $\theta_k(x) \sim x^{1/2}$ for flat-plate flow. For nonsimilar flows, we calculate it as a part of the solution at each streamwise station, although, for simplicity, it could also be prescribed.

Initial Conditions

Similarity principles may also be used to calculate an initial solution. In similar flow, all variables and $\theta_k(x)$ are of the form ax^ϕ along $\eta = y/\theta_k(x) = \text{const}$, and the power law behavior (ϕ) of each of the variables is known a priori. Since, by construction, streamwise grid lines lie along constant η, unknowns at one streamwise station are related to those at the previous station. For example, $u_{i+1,j} = u_{i,j}$, $\psi_{i+1,j} = \psi_{i,j}(x_{i+1}/x_i)^{1/2}$, and $\tau_{i+1,j} = \tau_{i,j}(x_{i+1}/x_i)^{-1/2}$ along $\eta = \text{const}$ for flat-plate flow. We calculate an initial solution by simply replacing variables at $y_{i,j}$ by those at $y_{i+1,j}$ with the appropriate scaling, thereby obtaining a closed system of equations. Transformation of the equations to similarity form is not necessary.

Results

Similar flow provides ideal test cases for comparison of the finite-volume scheme with conventional methods. Table 1 gives the nondimensional wall shear stress and displacement thickness for laminar flow over a flat plate, as calculated with Keller's box scheme (KBS) and the finite-volume scheme (FVS).

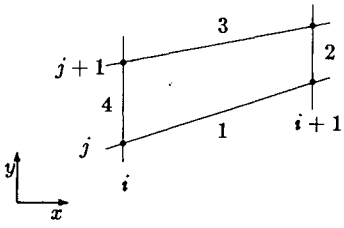

Fig. 1 Computational cell.

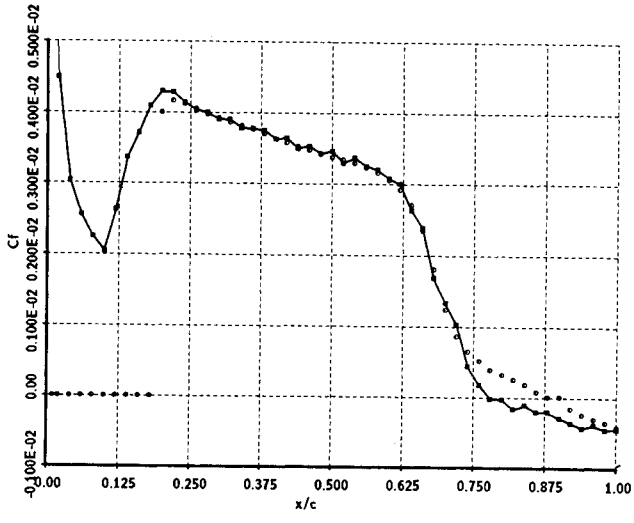

Fig. 2 Circular-arc airfoil: skin friction.

KBS wall shear results are somewhat more accurate than FVS shear results, but the finite-volume scheme predicts the displacement thickness more accurately than does KBS. The errors for both schemes decrease as the square of the grid spacing, indicating second-order-accurate discretizations.

Finally, we present results for a turbulent separated boundary layer on a bicircular-arc airfoil of 18% thickness ratio, at $M_\infty = 0.7425$, $Re_\infty = 4 \times 10^6$, and zero angle of attack. This flow case has been calculated previously as a viscous/inviscid coupling problem by Wigton and Holt.[2] The flow accelerates around the leading edge, goes through a weak shock at about 70% chord, decelerates, and separates just upstream of the trailing edge. Wigton and Holt[2] used a potential solver for the inviscid solution and Green's lag entrainment scheme in the boundary layer.

We pose the problem as a direct/inverse boundary condition problem, with edge velocity specified up to 68% chord and displacement thickness specified subsequently. The edge velocity due to Ref. 2 was calculated from the reported pressure distribution by assuming constant stagnation pressure. The displacement thickness was read directly from Ref. 2. The flow was assumed to undergo transition to turbulence linearly between $x/c = 0.1$ and 0.2, and 40 cells were used across the boundary layer.

Figure 2 gives the FVS skin-friction results as well as the skin friction given in Ref. 2. for $x/c > 0.2$. (Results for $x/c < 0.2$ are not given in Ref. 2.) Agreement with Wigton and Holt's results is excellent up to about 70% x/c, however, predictions of the separation point differ by about 5% x/c. It is not clear which of the methods is in error, but we note that the Cebeci-Smith turbulence model used in the finite-volume scheme is based on equilibrium boundary-layer assumptions, and is not valid near separation.

References

[1]Loyd, B. and Murman, E. M., "Finite Volume Solution of the Compressible Boundary Layer Equations," NASA CR 4013, 1986.

[2]Wigton, L. B. and Holt, M., "Viscous-Inviscid Interaction in Transonic Flow," *Proceedings of the AIAA 5th Computational Fluid Dynamics Conference*, 1981, pp. 77-89.